Breast Cancer: Targets and Therapy

Dovepress

open access to scientific and medical research

Open Access Full Text Article

ORIGINAL RESEARCH

Dosimetric Study and Robustness Analysis of Base Note Intensive Locked Field Radiotherapy for Left Breast Cancer

Chengqiong Tang[1], Qian Cao[2], Xiuqing Ai[2]

[1]Xinjiang Key Laboratory of Oncology, Department of Radiation Physics Technology, Xinjiang Uygur Autonomous Region Radiotherapy Clinical Research Center, Urumqi, Xinjiang Uyghur Autonomous Region, People's Republic of China; [2]Department of Breast Radiotherapy. The Affiliated Cancer Hospital of Xinjiang Medical University, Urumqi, Xinjiang Uyghur Autonomous Region, People's Republic of China

Correspondence: Xiuqing Ai, Department of Breast Radiotherapy, The Affiliated Cancer Hospital of Xinjiang Medical University, No. 789 Suzhou East Street, Urumqi, Xinjiang Uyghur Autonomous Region, 830000, People's Republic of China, Tel +86 13999852226, Email 2863223435@qq.com

Background: The locked vision plan can make the left breast cancer heart and lung organs dose.

Objective: The aim of the present study was to compare the dosimetric differences between field-locked and field-split plans in intensity-modulated radiotherapy for left-sided breast cancer, to explore the effect of field-locking on the low-dose region, and to evaluate its robustness to the radiotherapy target, in order to provide a reference for the selection of clinical radiotherapy protocols.

Methods: A total of 30 patients were selected after radical left breast cancer surgery, and 7-field locked-field and split-field plans were developed to compare the dose difference (ΔD) between the target area and each organ at risk, and to introduce offsets of 3, 5 and 7 mm in six directions and recalculate the perturbed dose distributions, and to compare the ΔD between the original and the perturbed plans according to the robustness of the plans.

Results: The results revealed that the $D_{98\%}$, $D_{95\%}$ and D_{mean} values of the planning target volume (PTV) of the two plans differed little and were not statistically different. The locked field plan provided better protection for the left lung, right lung, heart, right breast and left anterior descending coronary artery. For PTVΔ$D_{98\%}$, PTVΔ$D_{95\%}$, PTVΔD_{mean}, the ΔD was higher for the Locked Fields plan, and for LungLΔ5, LungLΔ20 and HeartΔ$_{mean}$, the ΔD was higher for the original plan.

Discussion: It was concluded that the field-locking plan could reduce the low-dose area of the affected lung and provide improved protection to the remaining critical organs, and the field-locking plan was more robust in protecting critical organs. Meanwhile, the field-locking plan showed higher sensitivity to positional deviation for target PTV.

Keywords: breast cancer, intensity-modulated radiotherapy, field-locking, low-metering, robustness

Introduction

Breast cancer is one of the most common malignant tumours in women, and radiotherapy is an important part of the comprehensive treatment of breast cancer.[1] Postoperative radiotherapy can effectively reduce the likelihood of local and regional lymph node recurrence. For patients with intermediate and advanced stage disease, adjuvant radiotherapy is usually needed to the lymphatic drainage area above and below the clavicle and to the breast area in the chest wall.[2] The number of fields and field angles used for treatment and fixed-field intensity tuning vary between investigators and extensive dosimetric comparisons have been made.[3] The prognosis of breast cancer is favorable, and the radiation carcinogenic effect after radiotherapy has attracted increasing attention. Michael H conducted an in-depth and systematic analysis of the articles published between 2006 and 2017, and concluded that low-dose radiation increases the risk of related tumors.[4] Pericarditis, valvular dysfunction, cardiomyopathy and coronary artery disease are some of the most severe advanced cardiotoxic effects that make the incidence of radiation-induced heart disease between 5% and 10% with in 10–30 years after irradiation.[5] Fixed tungsten door, which is the lead door, relies on the movement of the MLC to meet the optimal design. Fixed tungsten grating technology is an intensity modulation technique that can reduce leakage rays

Received: 22 November 2023
Accepted: 28 June 2024
Published: 30 July 2024

by locking multiple gratings, and the technique of intensity-modulated radiotherapy can limit the range of the field of view.[6] It is estimated that by following classic fractionated radiotherapy, the risk of cardiac mortality is <1% for 15 years when one-tenth of the whole heart volume receives less than 25 Gray (Gy),[7] and it could reduce the dose to the normal organs such as lung and heart in the radiotherapy of patients with breast cancer. Moreover, cardiac damage was found to be correlated with the heart-absorbed dose with 7.4% rate increase of ischemic heart disease per one Gy (95% confidence interval, 2.9–14.5; $P<0.001$), with no minimum threshold for risk.[8] Afifi et al[9] revealed that BC remains the main cause of death, and that heart disease may be an important cause of cancer-unrelated deaths. Due to the fact that the large coronary arteries are located deep in the heart, they increase linearly with the average dose to the heart.[10] Optimizing the dose distribution in the heart by fixing the tungsten gate, known as field-locking, can reduce radiation damage.[11–13]

There are many uncertainties in the planning and delivery of radiotherapy.[14,15] The intensity modulation technique is mainly based on the movement of the multileaf collimator (MLC) to achieve intensity modulation in the field, and the change in MLC position will have different effects on the target area and organs at risk. In the present study, a specific shot-field fixation tungsten gate intensity-modulated radiation therapy (IMRT) plan was designed separately from the split-field plan for patients after radical surgery for breast cancer with supraclavicular lymph node metastases.

The use of dose robustness and correlation of dose distributions in photon radiotherapy has been relatively little studied, with motion and uncertainty in radiotherapy leading to the onset of robustness. As the complexity of radiotherapy planning increases, the same applies to the need for plan robustness.[16] In the present study, focus was addressed on the effect of field-locking and field-splitting plans on the dose distribution to the target area and critical organs after radical left breast cancer surgery, as well as the introduction of offsets of 3, 5 and 7 mm in six directions and the recalculation of perturbed dose distributions. To compare the dose difference (ΔD) between the original and perturbed plans according to the robustness of the plan and to understand how the difference varies between the dose distribution to the target area and the dose distributions to the heart, lung, contralateral breast and other critical organs, they were irradiated with different dose volumes. In the present study, the advantages and disadvantages of the two plans and the sensitivity of these two modalities to positional shifts were investigated with the aim of providing a reference for clinical preference.

Materials and Methods

Case selection

These data are purely theoretical studies and have obtained informed consent from the study participants. The present study was approved (approval no. XJZ-LL-2019-001) by the Ethics Committee of The Affiliated Cancer Hospital of Xinjiang Medical University (Urumqi, China). A total of 30 patients who received adjuvant radiotherapy after radical mastectomy for breast cancer treated at The Affiliated Cancer Hospital of Xinjiang Medical University between January 2019 and May 2021 were retrospectively analyzed. The irradiation target area includes the chest wall and regional lymph nodes (RNI). Written informed consent was obtained from all patients. Patient characteristics are listed in Table 1.

Table 1 Clinical and Statistical Characteristics of the Patient Cohort

Patient	Age, years	PTV, cm^3	TNM stage
1	51	1082.37	T1cN1M0
2	39	871.58	T2N1M0
3	49	1010.92	T2N1M0
4	46	1008.13	T2N1M0
5	54	1090.21	T1N1M0
6	51	978.32	T1N1M0

(*Continued*)

Table 1 (Continued).

Patient	Age, years	PTV, cm^3	TNM stage
7	59	989.45	T1N1M0
8	44	898.56	T2N2M0
9	48	1115.12	T1N2M0
10	50	1045.32	T1N2M0
11	58	1215.08	T2N1M0
12	54	1023.45	T2N1M0
13	45	968.63	T2N2M0
14	43	1057.39	T1N2M0
15	57	895.97	T1N2M0
16	53	1068.46	T1N1M0
17	49	968.53	T2N1M0
18	52	1065.42	T1N1M0
19	48	895.76	T1N2M0
20	53	1067.43	T2N1M0
21	52	1075.39	T2N1M0
22	56	987.58	T1N2M0
23	49	995.43	T2N1M0
24	54	1056.46	T1N2M0
25	48	1023.65	T1N1M0
26	53	958.37	T1N2M0
27	46	1064.39	T2N1M0
28	51	1023.64	T1N2M0
29	48	985.47	T2N1M0
30	52	1053.76	T1N1M0

Abbreviation: PTV, planning target volume.

Position fixation and CT scanning

The position was fixed with a body membrane. Siemens Somatom Sensation 16-row spiral CT was performed in supine position. The scanning range is from chest Lower sternum to the level of tracheal protrusion (Figure 1). The irradiation technology adopts tangential IMRT.

Prescribing dose requirements

Post-scan CT images were transferred from the network to the Varian Eclipse 11.0 workstation, and all target areas and organs at risk were outlined by an experienced oncologist and reviewed and approved by a senior physician. Dosimetric evaluation for planning target volume (PTV) was $D_{95\%} \geq 50$ Gy, and the remaining observations were 95% dose coverage for PTV ($D_{95\%}$) and 98% dose coverage ($D_{98\%}$). $V_{30\ Gy}$, $V_{20\ Gy}$, $V_{5\ Gy}$, D_{mean} for the ipsilateral lung (Lung L) and $V_{5\ Gy}$,

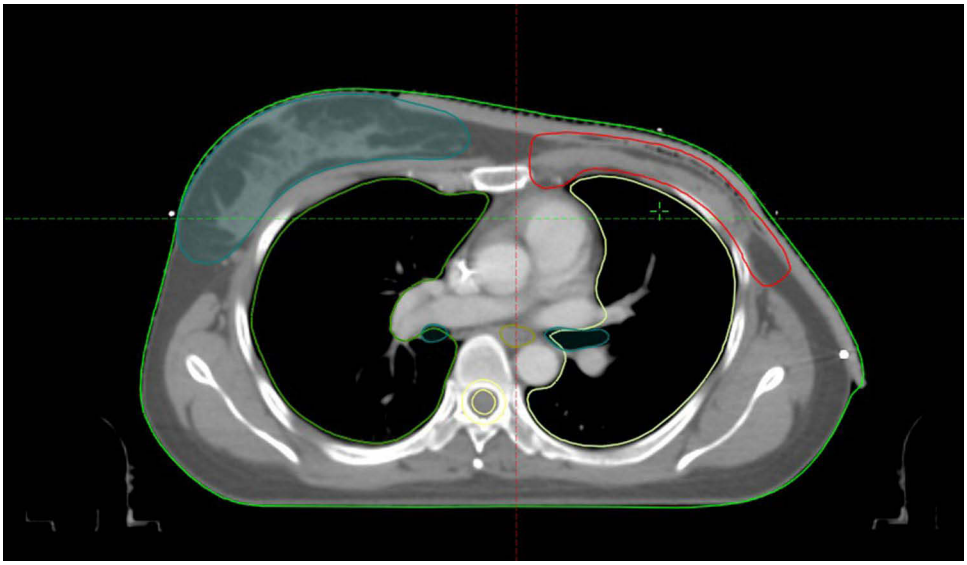

Figure 1 Example of CT scan of left breast cancer.
Abbreviation: CT, computed tomography.

D_{mean} for the heart, $V_{5\ Gy}$, D_{mean} for the contralateral lung (Lung R) and $V_{10\ Gy}$, D_{mean} for the contralateral breast (Breast R), as well as maximum dose (D_{max}) and mean dose (D_{mean}) for the left anterior descending coronary artery (LAD). Dx% denotes the dose received in Gy for x% of the volume, and VyGy denotes y Gy of the volume.

Plan design

All breast cancer plans were designed on a Varian Eclipse workstation. IMRT was delivered using six MV X-rays with a total of seven fields and fixed rack angles of 315, 330, 350, 10, 80, 105 and 120° (Figure 2). The plan design was performed on a VarianEclipse workstation. Appropriate optimization parameters were selected according to the physician's prescription dose requirements, lock-field means fixed tungsten door, which is the lead door, relies on the movement of the MLC to meet

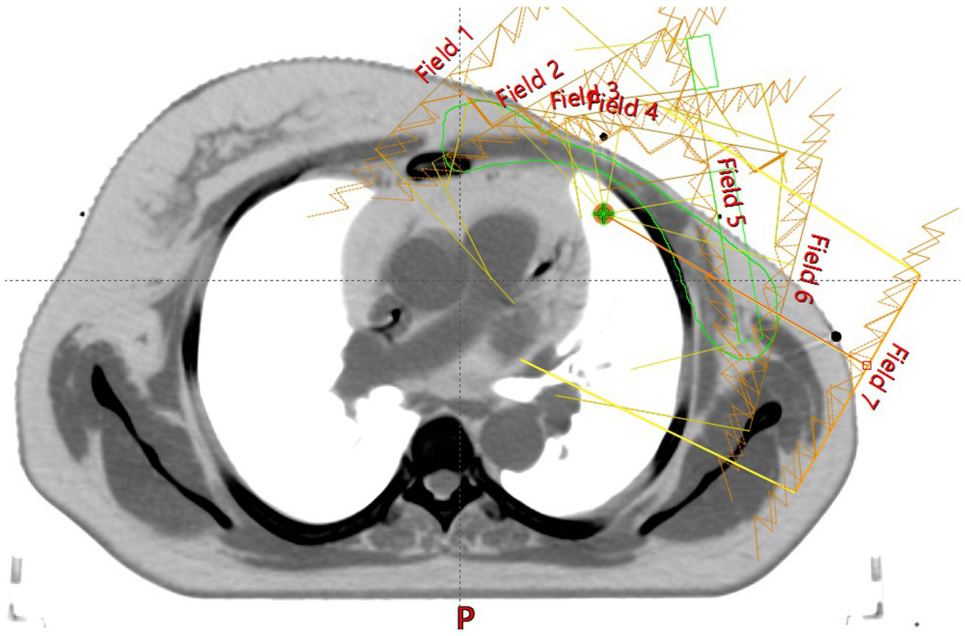

Figure 2 Intensity-modulated radiation therapy was delivered using 6 MV X-rays with a total of seven fields.

the optimal design, and the optimization parameters were guaranteed to remain constant throughout the design of the lock-field and split-field plans, with only the state of the MLC varying. Optimization objectives, convolutional optimization and iterative optimization were used, with the MLC angle set to zero for the sub-field plan. The field locking plan aims to avoid the affected lungs as much as possible, while ensuring that the target area on the direction of incidence of the field falls as much as possible within the irradiation field (boundary X ≤13.9 cm). The specific irradiation mode is shown in Figure 3.

Robustness quantification methods

In order to simulate the dose changes due to pendulum or systematic errors, 18 perturbed dose distributions were calculated for the 7-field locking plan and the 7-field splitting plan, respectively: the dose changes that should be induced by shifting the centre of the centre by ±3, ±5 and ±7 mm, respectively, from its reference point in the up-down (S-I), left-right (L-R), and anterior-posterior (A-P) directions. In the present study, dose-volume histogram (DVH) was used as a robust quantification method and the dosimetric parameters in both plans are shown in the DVH curves. Differences in dosimetric parameters (ΔDx% and ΔVy-Gy) were used for calculations, and values with smaller differences indicated improved robustness.

Statistical analyses

SPSS (version 20.0; IBM Corp) was used for statistical analysis. Non-parametric Wilcoxon signed rank test was used for data that did not fit the normal distribution, and paired sample *t*-test was used for data that fit the normal distribution. *T*-tests were used for those that conform to normal distribution, and paired sample non-parametric tests were used for those that do not conform to normal distribution.

Results

Dose distribution in target areas and organs at risk

The dose distribution in each target area for both the field-locking and field-splitting plans meets the clinical requirements. The $D_{98\%}$, $D_{95\%}$ and D_{mean} of each PTV differed little ($P \geq 0.05$), as shown in Table 2.

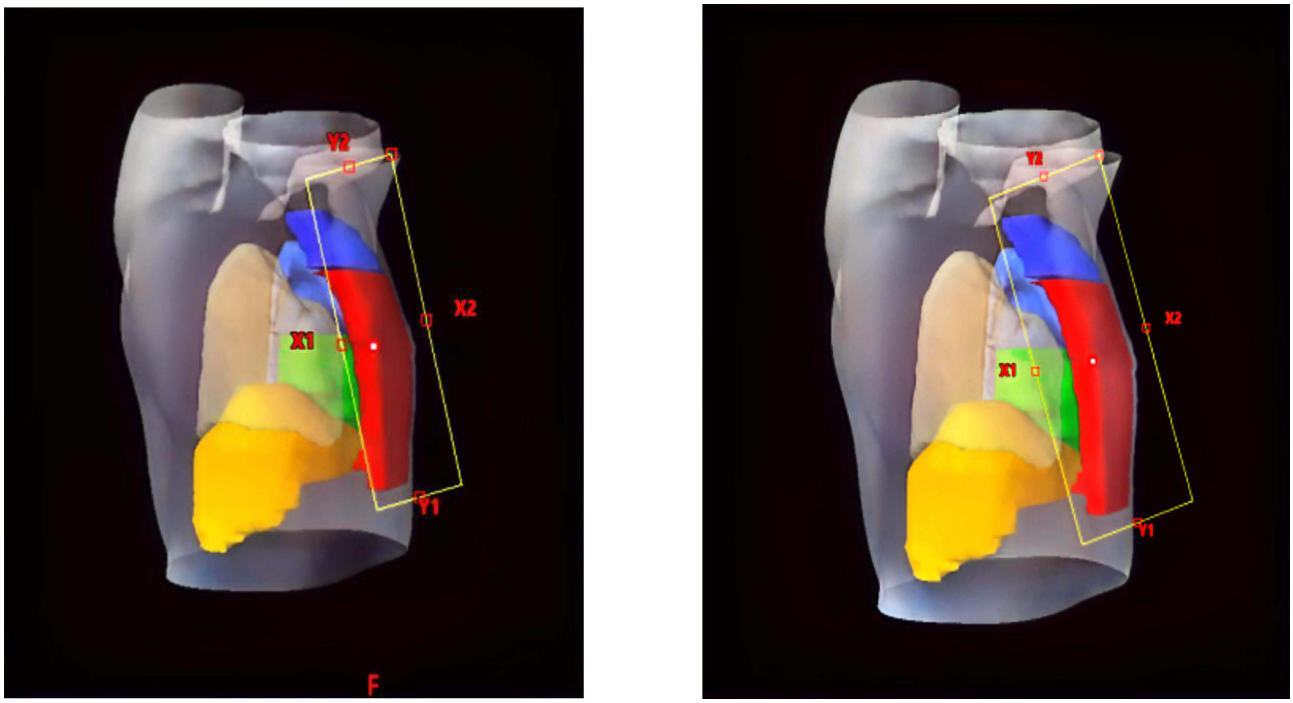

Figure 3 Lock field shooting mode and Div field plan shooting mode.

Table 2 Dosimetric Parameters of $D_{98\%}$, $D_{95\%}$ and D_{mean} of 30 Patients with Normal PTV in 7F-Locked Field Plan and 7F-Dividing Field Plan

Target area	Evaluated items	7F-Locked Field plan (Gy)	7F-Dividing Field plan (Gy)	t/Z[a]	*P*-value
PTV	$D_{98\%}$	49.42 (49.13–49.47)	49.47 (49.07–49.51)	−1.060[a]	0.289
PTV	$D_{95\%}$	50.07 (49.96–50.08)	50.21 (50.04–50.24)	−1.948[a]	0.051
PTV	D_{mean}	51.02±0.45	51.01±0.54	0.086	0.932

Notes: Means are expressed as the mean ± standard deviation for those that conform to normal distribution and median M50 (M25-M75) for those that do not. [a]z-value.
Abbreviation: PTV, planning target volume; Gy, Gray; $D_{98\%}$, dose contained in 98% of the volume; $D_{95\%}$, dose contained in 98% of the volume; D_{mean}, average dose.

For left lung V_5, V_{20} and D_{mean}, the field-locking plan was lower than the field-splitting plan, and the difference was statistically significant; for right lung V_5 and D_{mean}, heart V_5 and D_{mean}, right breast D_{mean} and LAD the field-locking plan was lower than the field-splitting plan, and the difference was statistically significant (all $P<0.05$), as shown in Table 3.

Plan robustness evaluation

A plan robustness quantification method is used where ΔD is calculated, and corresponds to the plan robustness of the structure. The dose volume changes for PTVΔ$D_{98\%}$, PTVΔ$D_{95\%}$ and PTVΔD_{mean} when introducing positional offsets in the six directions are demonstrated in Figures 4–6. PTVΔ$D_{98\%}$, Δ$D_{95\%}$ and ΔD_{mean} are shown in Table 4.

PTVΔ$D_{98\%}$ (L3, P3, S3, I3, L5, P5, I5, S7, I7), the ΔD of the lock-field plan was markedly larger, the robustness needs to be improved and the difference was statistically significant (P<0.05). PTVΔ$D_{95\%}$ (L3 mm, R3, A3, P3, S3, I3, L5, A5, P5, I5, L7, R7, P7, S7) variations in the dose of the lock-field program were more variable, with greater

Table 3 Dosimetric Parameters of Lung L, Lung R, Heart, Breast R and LAD in 30 Patients

OAR	Evaluated items	7F-Locked field plan (%/Gy)	7F-Dividing Field Plan (%/Gy)	t/Z[a]	*P*-value
Lung L	V_{30Gy}	12.87±1.42	12.54±1.44	1.922	0.064
	V_{20Gy}	20.43±1.40	21.04±1.28	−3.170	0.004
	V_{5Gy}	56.70±4.42	64.23±6.34	−13.165	<0.0001
	D_{mean}	11.86±0.87	12.35±0.70	−4.005	<0.0001
Lung R	V_{5Gy}	5.62±1.74	8.20±3.58	−6.254	<0.0001
	D_{mean}	2.18 (2.09–2.45)	2.56 (2.47–2.99)	−4.320[a]	<0.0001
Heart	V_{5Gy}	35.97 (35.19–41.13)	49.59 (47.07–56.09)	−5.295[a]	<0.0001
	D_{mean}	6.43±0.71	7.46±0.67	−10.771	<0.0001
Breast R	V_{10Gy}	7.50 (6.75–8.06)	7.54 (7.43–9.89)	−2.373[a]	0.018
	D_{mean}	4.57 (4.38–4.70)	5.34 (4.94–5.45)	−4.564[a]	<0.0001
LAD	D_{max}	36.17±2.22	36.26±2.27	−0.181	0.858
	D_{mean}	24.45±1.19	25.08±1.11	−4.164	<0.0001

Notes: Means are expressed as the mean ± standard deviation for those that conform to normal distribution and median M50 (M25-M75) for those that do not; [a]z-value.
Abbreviations: Gy, Gray; LAD, left anterior descending coronary artery; OAR, organs at risk; R, contralateral; L, ipsilateral; V_{30Gy}, volume of 30 Gy when receiving the dose; V_{20Gy}, volume of 20 Gy when receiving the dose; V_{5Gy}, volume of 5 Gy when receiving the dose; D_{mean}, average dose.

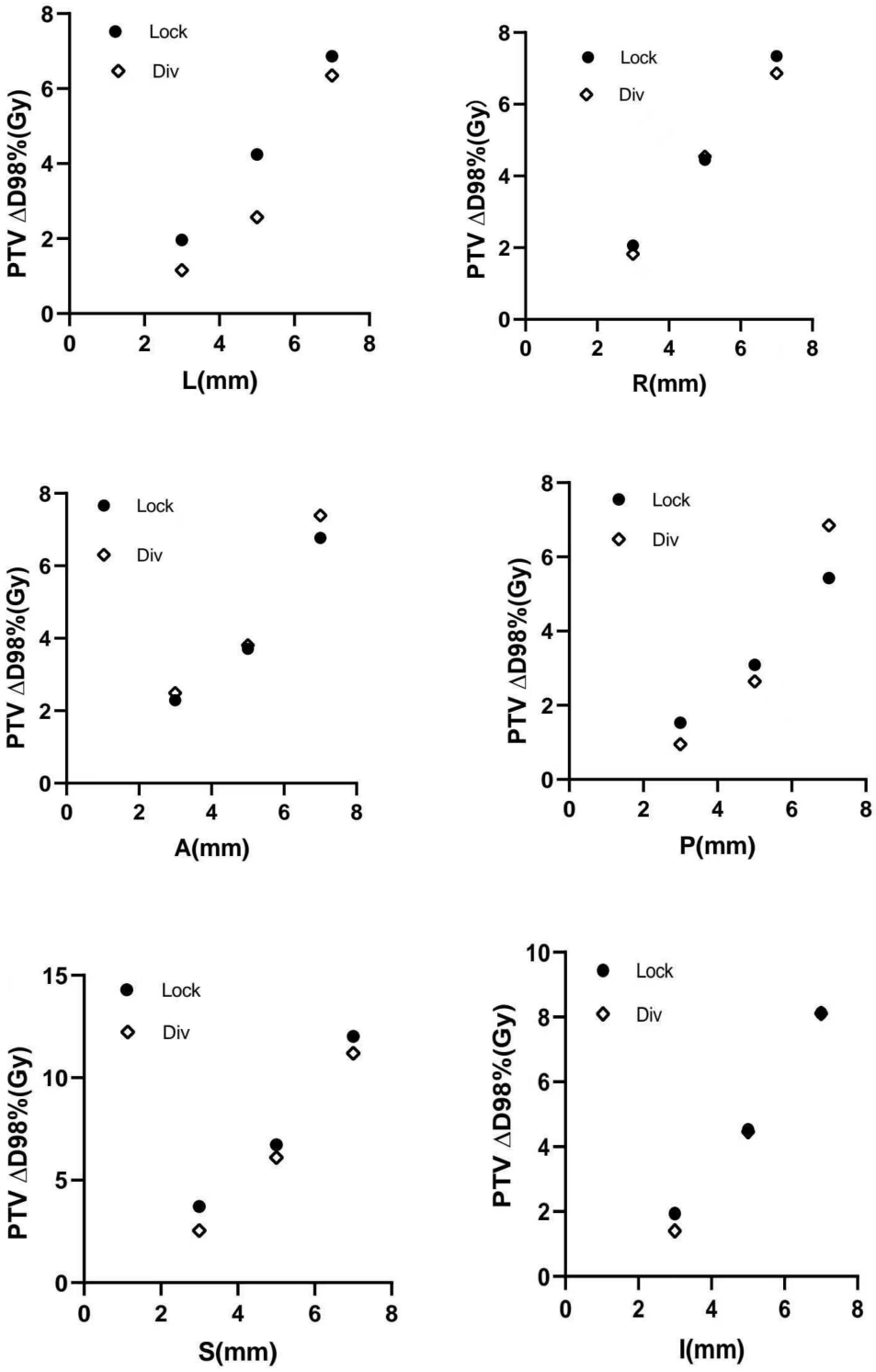

Figure 4 Dose difference of PTV $\Delta D_{98\%}$ between the reference and perturbed 7F- Lock IMRT and 7F-Div-IMRT plans for different isocenter shifts. Black dots indicate 7F Lock Field plans; square boxes indicate 7F-Div-IMRT plans.
Abbreviations: IMRT, intensity-modulated radiation therapy; PTV, planning target volume.

robustness to be improved and a statistically significant difference (P<0.05). In the $PTVD_{mean}$ (L3, P3, S3, I3, L5, R5, A5, P5, S5, L7, R7, A7, S7), the variation in the change in the dose of the lock-field plan was greater, the robustness needs to be improved, and the difference was statistically significant (P<0.05).

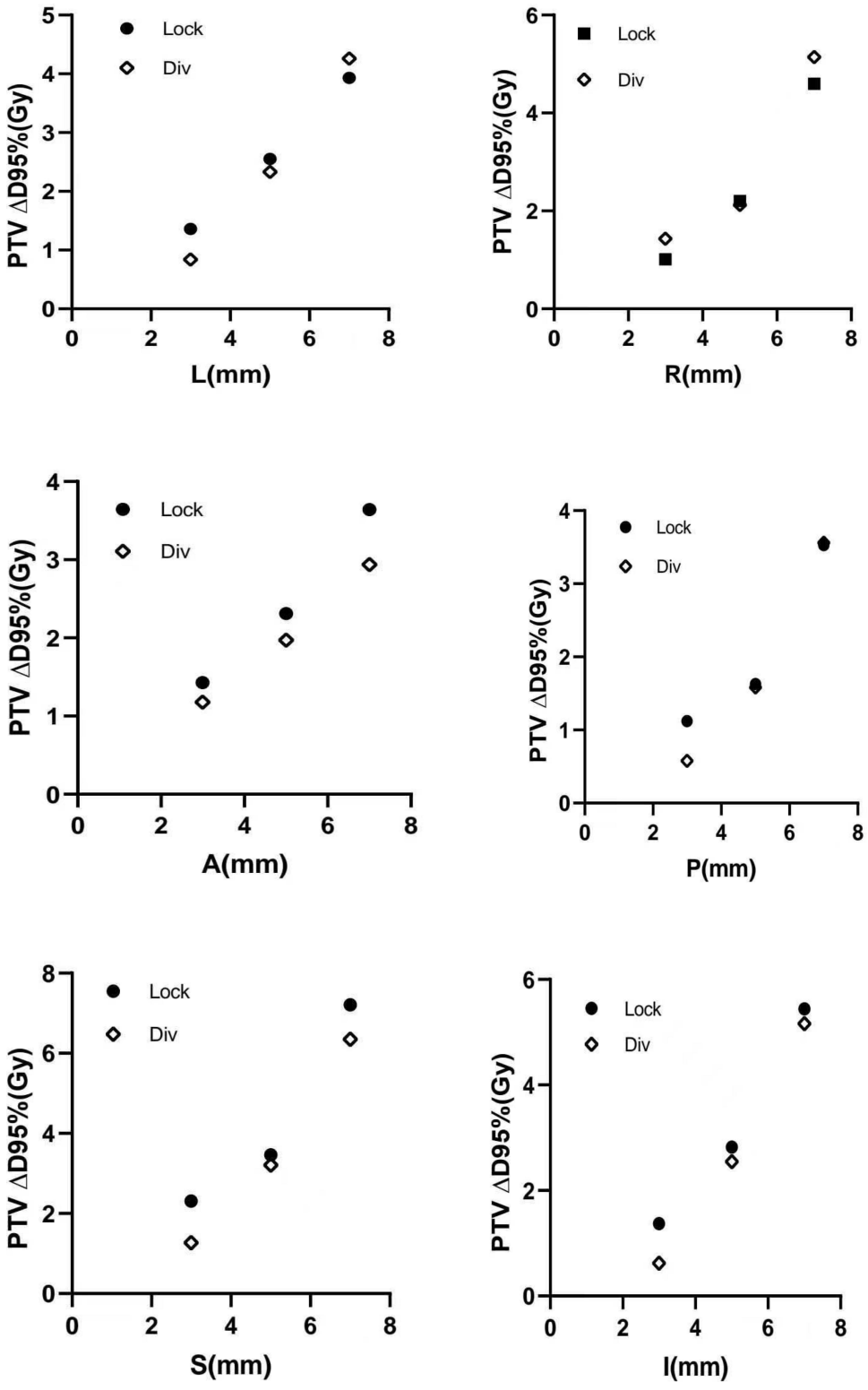

Figure 5 Dose difference of PTV $\Delta D_{95\%}$ between the reference and perturbed 7F- Lock IMRT and 7F-Div-IMRT plans for different isocenter shifts. Black dots indicate 7F Lock Field plans; square boxes indicate 7F-Div-IMRT plans.
Abbreviations: IMRT, intensity-modulated radiation therapy; PTV, planning target volume.

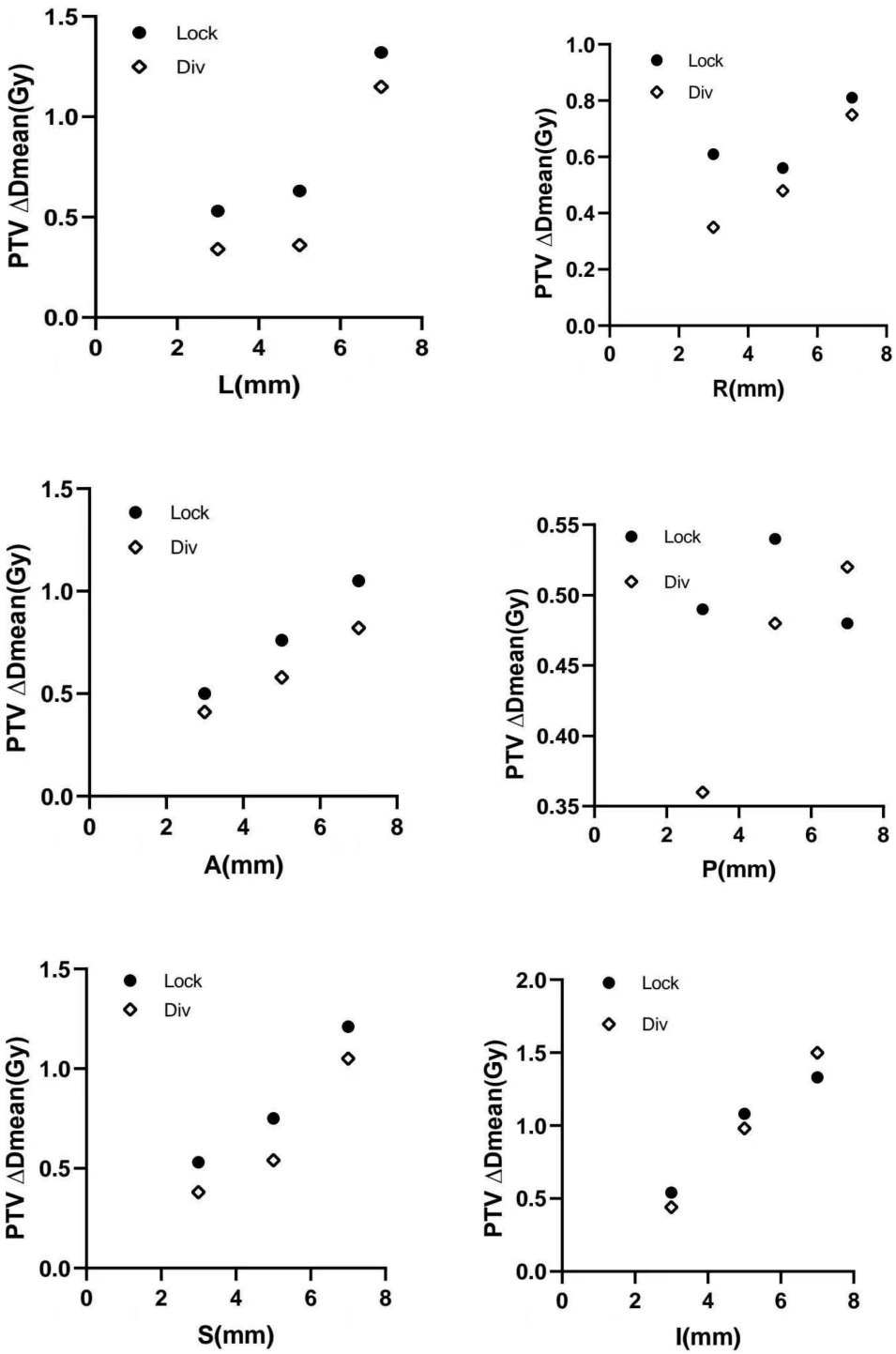

Figure 6 Dose difference of PTV ΔD_{mean} between the reference and perturbed 7F- Lock IMRT and 7F-Div-IMRT plans for different isocenter shifts. Black dots indicate 7F Lock Field plans; square diamond boxes indicate 7F-Div-IMRT plans.
Abbreviations: IMRT, intensity-modulated radiation therapy; PTV, planning target volume.

In Lung L Δ5 (L3, R3, P3, I3, L5, P5, S5, I5, L7, P7), Lung L Δ20 (L3, P3, L5, P5, L7, P7) and HeartΔ_{mean} (I3, L5, P5, S5, L7) were smaller than the split-field plan, the robustness of the locked-field plan was improved, and the difference was statistically significant (P<0.05), as revealed in Figures 7–9 and Table 5.

Table 4 Dosimetric Differences Between the Two Plans After Moving the PTV in All Directions

PTV	Evaluated items (mm)	7F-Locked Field plan (%/Gy)	7F-Dividing Field Plan (%/Gy)	t/Z[a] value	*P*-value
$\Delta D_{98\%}$ (Gy)	L (3)	1.97 (1.85–2.09)	1.21 (0.99–1.43)	−4.618[a]	<0.0001
	R (3)	2.02 (1.75–2.29)	1.84 (1.57–2.11)	−0.968[a]	0.333
	A (3)	2.25±0.61	2.52±1.03	7.279	<0.0001
	P (3)	1.55 (1.45–1.66)	0.98 (0.81–1.15)	−3.877[a]	<0.0001
	S (3)	3.72 (3.39–4.06)	2.59 (2.19–2.99)	−4.741[a]	<0.0001
	I (3)	1.96 (1.80–2.11)	1.37 (1.22–1.52)	−4.395[a]	<0.0001
	L (5)	4.35±1.03	2.75±1.20	−2.634	0.013
	R (5)	4.34 (3.93–4.77)	4.70 (4.03–5.38)	−0.483[a]	0.629
	A (5)	3.71 (3.61–3.82)	3.93 (3.56–4.30)	−0.148[a]	0.882
	P (5)	3.11 (2.86–3.36)	2.64 (2.30–2.98)	−3.559[a]	<0.0001
	S (5)	6.57±1.61	6.30±1.64	1.655	0.109
	I (5)	4.69 (4.44–4.94)	3.72 (3.27–4.17)	−3.816[a]	<0.0001
	L (7)	6.82 (6.32–7.31)	6.42 (5.95–6.89)	−1.306[a]	0.191
	R (7)	7.46 (6.89–8.02)	7.17 (6.57–7.77)	−1.337[a]	0.181
	A (7)	6.89 (6.74–7.04)	7.51 (7.00–8.03)	−2.487[a]	0.013
	P (7)	5.77 (5.37–6.17)	6.19 (5.66–6.72)	−2.283[a]	0.022
	S (7)	11.61 (11.28–11.94)	10.79 (10.17–11.41)	−3.587[a]	<0.0001
	I (7)	8.10 (7.73–8.47)	6.97 (6.46–7.49)	−3.157[a]	0.002
$\Delta D_{95\%}$ (Gy)	L (3)	1.38 (1.30–1.45)	0.83 (0.68–0.97)	−4.135[a]	<0.0001
	R (3)	1.42 (1.34–1.49)	1.03 (0.94–1.13)	−4.207[a]	<0.0001
	A (3)	1.25 (1.16–1.34)	1.06 (0.94–1.18)	−2.995[a]	0.003
	P (3)	1.10 (1.04–1.17)	0.57 (0.49–0.66)	−4.639[a]	<0.0001
	S (3)	2.64±0.46	1.22±0.36	13.197	<0.0001
	I (3)	1.38 (1.34–1.43)	0.66 (0.54–0.78)	−4.680[a]	<0.0001
	L (5)	2.44 (2.24–2.64)	2.00 (1.81–2.18)	−3.692[a]	<0.0001
	R (5)	2.00 (1.66–2.36)	2.12 (1.83–2.40)	−0.505[a]	0.614
	A (5)	2.24±0.36	1.91±0.28	7.236	<0.0001
	P (5)	1.78 (1.68–1.89)	1.57 (1.48–1.66)	−2.705[a]	0.007
	S (5)	3.50 (3.26–3.75)	3.42 (3.21–3.63)	−1.183[a]	0.237
	I (5)	2.91 (2.74–3.07)	2.20 (1.95–2.44)	−3.970[a]	<0.0001
	L (7)	4.04 (3.74–4.34)	3.76 (3.42–4.10)	−2.098[a]	0.036
	R (7)	5.16±1.16	4.52±1.02	3.996	<0.0001
	A (7)	3.78 (3.49–4.08)	3.62 (3.20–4.05)	−1.769[a]	0.077

(*Continued*)

Table 4 (Continued).

PTV	Evaluated items (mm)	7F-Locked Field plan (%/Gy)	7F-Dividing Field Plan (%/Gy)	*t*/*Z*[a] value	*P*-value
	P (7)	3.51 (3.31–3.71)	3.27 (3.07–3.47)	−1.979[a]	0.048
	S (7)	7.04 (6.78–7.29)	6.78 (6.48–7.08)	−2.427[a]	0.015
	I (7)	5.28 (4.76–5.79)	5.44 (5.05–5.84)	−1.121[a]	0.262
ΔD_{mean} (Gy)	L (3)	0.54 (0.48–0.60)	0.37 (0.34–0.41)	−3.984[a]	<0.0001
	R (3)	0.59 (0.53–0.64)	0.36 (0.30–0.42)	−4.784[a]	<0.0001
	A (3)	0.48 (0.40–0.56)	0.41 (0.38–0.45)	−1.925[a]	0.054
	P (3)	0.50±0.13	0.37±0.10	4.763	<0.0001
	S (3)	0.50 (0.44–0.56)	0.31 (0.26–0.36)	−4.660[a]	<0.0001
	I (3)	0.56 (0.51–0.60)	0.45 (0.41–0.48)	−3.115[a]	0.002
	L (5)	0.65 (0.59–0.71)	0.51 (0.44–0.58)	−3.375[a]	0.001
	R (5)	0.63 (0.56–0.70)	0.47 (0.40–0.55)	−3.255[a]	0.001
	A (5)	0.78±0.26	0.59±0.18	6.290	<0.0001
	P (5)	0.63 (0.58–0.67)	0.48 (0.43–0.52)	−3.940[a]	<0.0001
	S (5)	0.74 (0.68–0.80)	0.64 (0.50–0.77)	−2.995[a]	0.003
	I (5)	1.06 (0.99–1.12)	1.03 (0.90–1.16)	−1.481[a]	0.139
	L (7)	1.06 (0.95–1.16)	0.93 (0.81–1.05)	−2.140[a]	0.032
	R (7)	0.94 (0.85–1.03)	0.81 (0.69–0.93)	−3.191[a]	0.001
	A (7)	1.03 (0.91–1.15)	0.86 (0.74–0.97)	−3.858[a]	<0.0001
	P (7)	0.49 (0.39–0.59)	0.55 (0.46–0.63)	−0.885[a]	0.376
	S (7)	1.20 (1.15–1.26)	1.05 (0.99–1.11)	−4.499[a]	<0.0001
	I (7)	1.34 (1.27–1.41)	1.43 (1.31–1.55)	−1.430[a]	0.153

Notes: Means are expressed as the mean ± standard deviation for those that conform to normal distribution and median M50 (M25-M75) for those that do not; [a]z-value.
Abbreviations: S, up; I, down; L, left; R, right; A, anterior; P, posterior; Gy, Gray; PTV, planning target volume.

Discussion

Although the focus is on the survival of patients with breast cancer, the potentially harmful effects of radiation caused by medical imaging need to be investigated further.

In order to reduce the image caused by low doses, a locking field calculation method was used, where the fixed locking technique refers to locking the lead gate; the lock field plan has been widely used in radiotherapy for nasopharyngeal, rectal, cervical and gastric cancer. If the size of the lead gate is not set properly in the intensity tuning plan, it may cause a certain loss of the irradiated dose to the target area as well as to the critical organs.[17–19] In the present study, the field-locking method was mainly used to investigate the effects of field-locking and field-splitting breast cancer IMRT plans on the dose to the target area and critical organs, and it was found that the $D_{98\%}$, $D_{95\%}$ and D_{mean} values of the target area (PTV) of the two plans had little difference and were not statistically different, which indicated that there was not marked variability between the two techniques in fulfilling the dose distribution to the target area. Adjuvant radiotherapy for patients with left breast cancer is associated with an increased risk of cardiac injury.[20,21] The magnitude of this risk is directly proportional to the average dose to the heart.[22,23] In addition, the design of the field-locking intensity adjustment technique for breast cancer patients in the present study yielded lower V_5, V_{20} and D_{mean} for the left

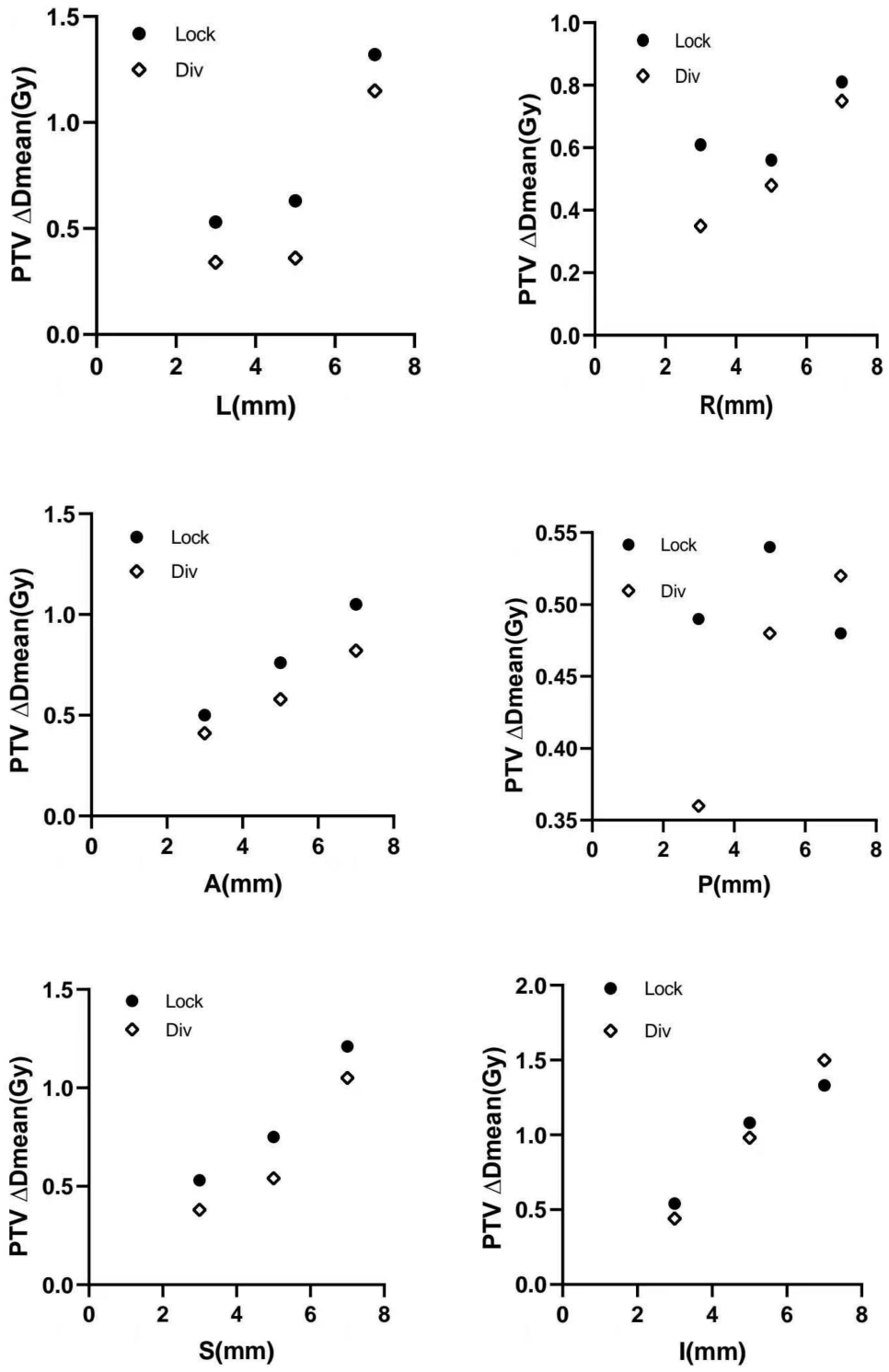

Figure 7 Dose difference of Lung L ΔV_5 between the reference and perturbed 7F- Lock IMRT and 7F-Div-IMRT plans for different isocenter shifts. Black dots indicate 7F Lock Field plans; square boxes indicate 7F-Div-IMRT plans. IMRT, intensity-modulated radiation therapy; PTV, planning target volume.

lung; V_5, D_{mean} for the right lung; V_5, D_{mean} for the heart; and D_{mean} for the right breast in the field-locking plan than in the field-splitting plan, and the difference was statistically significant, which suggested that the field-locking plan can reduce the low-dose region of the left lung to reduce the leakage of the radiation, while fulfilling the clinically required

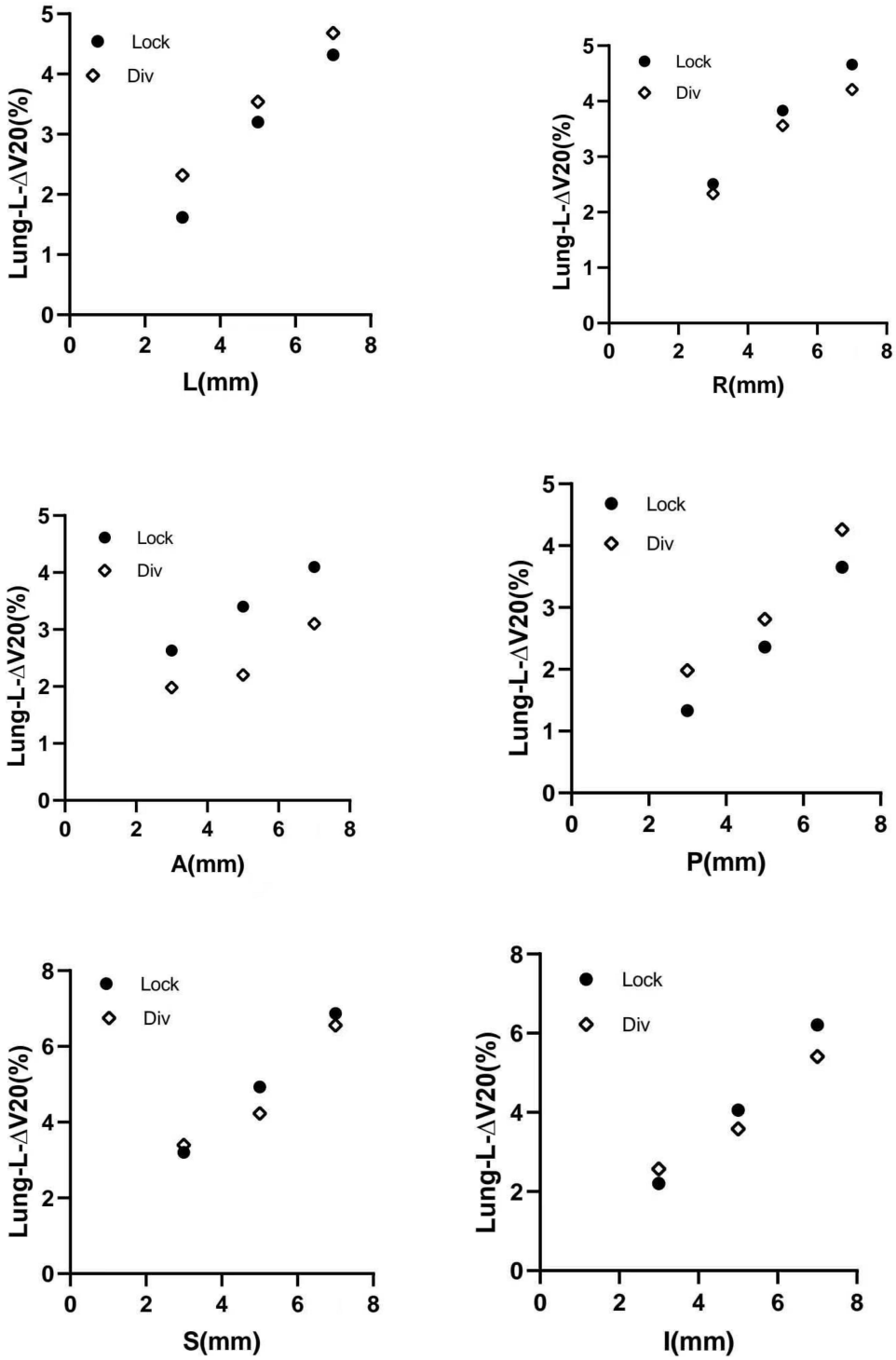

Figure 8 Dose difference of Lung L ΔV_{20} between the reference and perturbed 7F- Lock IMRT and 7F-Div-IMRT plans for different isocenter shifts. Black dots indicate 7F Lock Field plans; square boxes indicate 7F-Div-IMRT plans.

target-area coverage. The LAD dose, on the other hand, did not change significantly, probably due to the relatively small volume, which could not benefit from the Lock fields.

The study contrasts intensity-modulated radiotherapy plans for left-sided breast cancer, finding minimal differences in D98%, D95% and Dmean values of the planning target volume (PTV) between field-locked and field-split plans。The

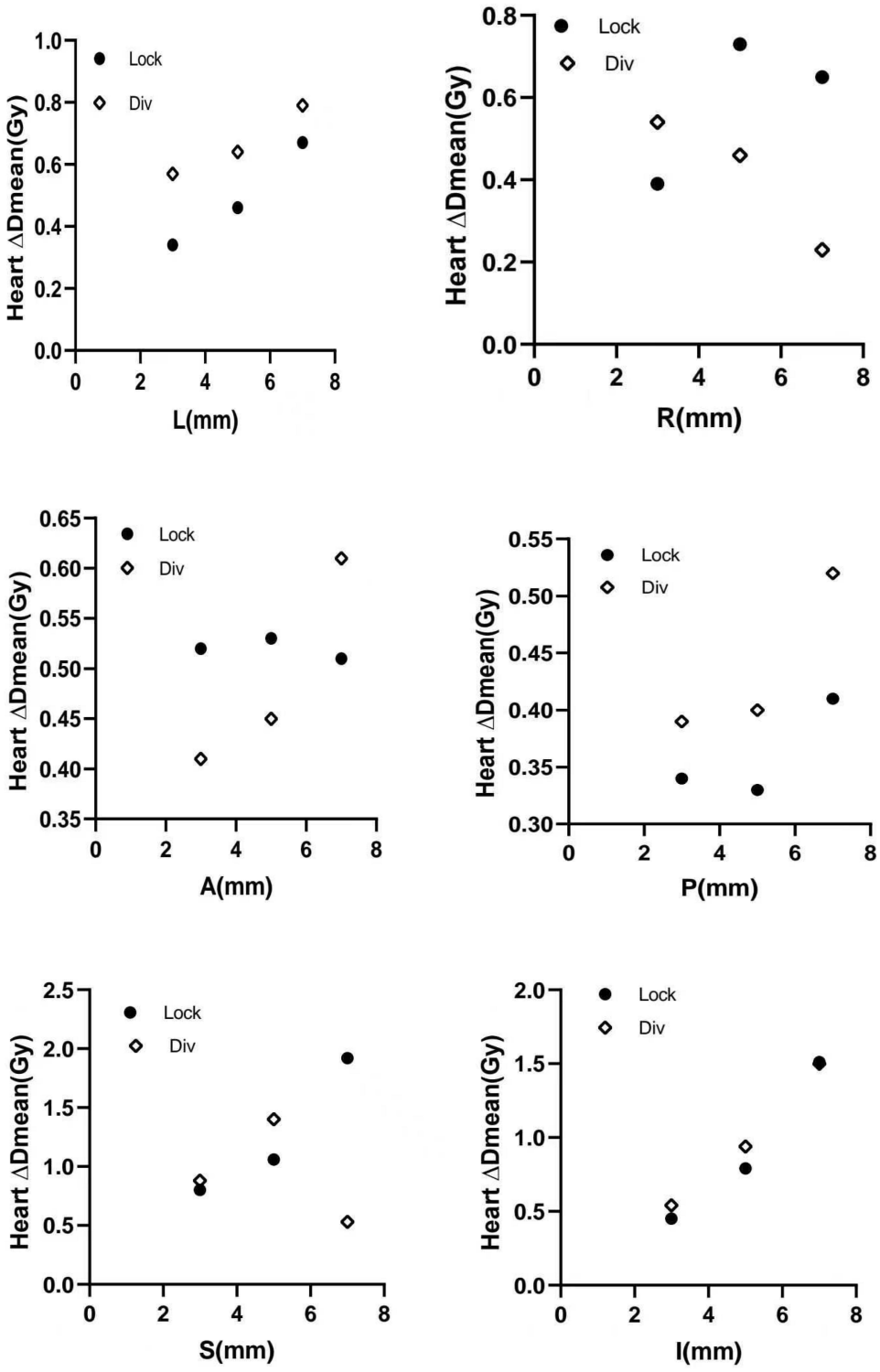

Figure 9 Dose difference of Heart ΔD_{mean} between the reference and perturbed 7F- Lock IMRT and 7F-Div-IMRT plans for different isocenter shifts. Black dots indicate 7F Lock Field plans; square boxes indicate 7F-Div-IMRT plans.
Abbreviations: IMRT, intensity-modulated radiation therapy.

field-locking plan excels in safeguarding critical organs-left lung, right lung, heart, right breast, and left anterior descending coronary artery. Notably, it reduces the low-dose region in the left lung, mitigating radiation leakage.

Despite organ protection benefits, the field-locked plan displays heightened sensitivity to positional deviation for the target PTV. Robustness analyses reveal larger variations in PTV dose metrics, highlighting potential stability challenges during dose

Table 5 Dosimetric Difference Statistics Between the 7F-Locked Field Plan and the 7F-Dividing Field Plan of OARS After Moving in All Directions

OARS	Evaluated items (mm)	7F-Locked field plan (%/Gy)	7F-Dividing Field Plan (%/Gy)	*t*/*Z*[a] value	*P*-value
Lung L-Δ V5	L (3)	3.08 (2.63–3.54)	4.39 (3.80–4.98)	−3.980[a]	<0.0001
	R (3)	2.50 (2.14–2.86)	4.52 (3.89–5.57)	−3.817[a]	<0.0001
	A (3)	4.78 (4.09–5.47)	3.51 (2.87–4.15)	−2.799[a]	0.005
	P (3)	2.67 (2.36–2.97)	4.18 (3.58–4.77)	−4.143[a]	<0.0001
	S (3)	5.06±1.11	5.03±2.27	0.082	0.935
	I (3)	1.07 (0.89–1.26)	2.88 (2.49–3.28)	−4.784[a]	<0.0001
	L (5)	2.87 (2.25–3.49)	4.07 (3.51–4.63)	−4.792[a]	<0.0001
	R (5)	3.52 (2.79–4.24)	3.72 (3.22–4.22)	−0.649[a]	0.516
	A (5)	4.33 (3.82–4.84)	4.20 (3.39–5.00)	−0.710[a]	0.478
	P (5)	1.70 (1.33–2.07)	2.70 (2.29–3.10)	−4.159[a]	<0.0001
	S (5)	5.06 (4.43–5.68)	6.16 (5.59–6.73)	−3.873[a]	<0.0001
	I (5)	0.89 (0.78–1.00)	2.31 (1.90–2.72)	−4.625[a]	<0.0001
	L (7)	3.70 (2.93–4.46)	4.73 (3.89–5.57)	−3.308[a]	<0.0001
	R (7)	3.93 (3.36–4.49)	3.12 (2.85–3.39)	−1.659[a]	0.097
	A (7)	4.92 (4.42–5.43)	4.31 (3.40–5.22)	−1.759[a]	0.079
	P (7)	1.39 (1.08–1.70)	3.38 (2.99–3.76)	−4.732[a]	<0.0001
	S (7)	8.09 (7.68–8.50)	8.61 (7.56–9.66)	−1.039[a]	0.299
	I (7)	3.76 (3.18–4.34)	2.87 (2.02–3.71)	−1.615[a]	0.106
Lung L-ΔV20	L (3)	1.55±0.60	2.41±1.11	−4.461	<0.0001
	R (3)	2.56 (2.26–2.86)	2.35 (1.96–2.74)	−1.516[a]	0.130
	A (3)	2.63 (2.22–3.04)	1.89 (1.47–2.31)	−2.986[a]	0.003
	P (3)	1.43 (1.21–1.65)	1.97 (1.61–2.33)	−2.456[a]	0.014
	S (3)	3.39 (3.10–3.67)	2.63 (2.12–3.14)	−3.031[a]	0.002
	I (3)	2.27±0.58	2.63±1.31	−1.411	0.169
	L (5)	3.23±0.90	3.53±1.33	−2.275	0.003
	R (5)	3.84 (3.60–4.09)	3.63 (3.05–4.21)	−0.985[a]	0.324
	A (5)	3.43 (3.06–3.80)	2.97 (2.44–3.49)	−2.096[a]	0.036
	P (5)	2.40 (2.17–2.63)	2.87 (2.48–3.27)	−2.430[a]	0.015
	S (5)	4.70 (4.36–5.04)	4.06 (3.44–4.68)	−2.771[a]	0.006
	I (5)	3.96 (3.62–4.29)	3.63 (3.28–3.98)	−1.505[a]	0.137
	L (7)	4.37 (3.89–4.85)	4.78 (4.19–5.36)	−2.144[a]	0.032
	R (7)	4.58 (4.35–4.82)	4.01 (3.60–4.42)	−3.021[a]	0.003
	A (7)	4.15 (3.85–4.45)	3.53 (3.00–4.07)	−2.727[a]	0.006

(*Continued*)

Table 5 (Continued).

OARS	Evaluated items (mm)	7F-Locked field plan (%/Gy)	7F-Dividing Field Plan (%/Gy)	*t*/*Z*[a] value	*P*-value
	P (7)	3.72 (3.54–3.90)	4.22 (3.80–4.65)	−2.596[a]	0.009
	S (7)	6.89 (6.34–7.44)	6.64 (5.85–7.44)	−0.906[a]	0.365
	I (7)	6.03 (5.54–6.52)	5.45 (5.07–5.83)	−2.428[a]	0.015
HeartΔD_{mean}	L (3)	0.31 (0.27–0.35)	0.33 (0.25–0.41)	−0.679[a]	0.497
	R (3)	0.41 (0.33–0.50)	0.54 (0.40–0.67)	−1.157[a]	0.247
	A (3)	0.53 (0.46–0.59)	0.42 (0.36–0.48)	−3.757[a]	<0.0001
	P (3)	0.34 (0.31–0.37)	0.42 (0.36–0.44)	−2.852[a]	0.004
	S (3)	0.80 (0.66–0.95)	0.89 (0.80–0.99)	−1.162[a]	0.245
	I (3)	0.45 (0.37–0.53)	0.52 (0.43–0.61)	−2.694[a]	0.007
	L (5)	0.46 (0.42–0.50)	0.62 (0.54–0.71)	−4.304[a]	0.000
	R (5)	0.83 (0.68–1.01)	0.57 (0.37–0.78)	−0.714[a]	0.475
	A (5)	0.53 (0.47–0.59)	0.47 (0.38–0.56)	−1.163[a]	0.245
	P (5)	0.34±0.18	0.40±0.16	−3.935	<0.0001
	S (5)	1.03±0.45	1.41±0.26	−4.564	<0.0001
	I (5)	0.77 (0.59–0.96)	0.92 (0.64–1.19)	−1.103[a]	0.270
	L (7)	0.68±0.14	0.81±0.24	−3.954	<0.0001
	R (7)	0.84 (0.68–1.01)	0.57 (0.37–0.78)	−3.90[a]	<0.0001
	A (7)	0.51 (0.41–0.60)	0.60 (0.50–0.71)	−2.799[a]	0.005
	P (7)	0.71 (0.54–0.88)	0.49 (0.34–0.53)	−1.420[a]	0.156
	S (7)	1.95 (1.88–2.02)	0.97 (0.69–1.26)	−4.598[a]	<0.0001
	I (7)	1.45 (1.21–1.69)	1.40 (1.07–1.73)	−1.111[a]	0.267

Notes: Means are expressed as the mean ± standard deviation for those that conform to normal distribution and median M50 (M25-M75) for those that do not; [a]z-value.
Abbreviations: S, up; I, down; L, left; R, right; A, anterior; P, posterior; OARs, organs at risk.

execution. However, whether there is a difference in the robustness of the field-locking plan compared with the original plan was also the focus of the current study; robustness considers the uncertainty during treatment and posing, and robustness is investigated to minimize instability during dose execution.[24,25] For the variation of PTV $\Delta D_{98\%}$, $\Delta D_{95\%}$ and ΔD_{mean}, the field-locking plan was larger than the field-splitting plan, and the difference was statistically significant, with larger values indicating poorer robustness. The field-locked plan was smaller than the field-split plan for changes in Lung L Δ_5, Lung L Δ_{20} and Heart Δ_{mean}, and the difference was statistically significant, indicating that the advantages of the field-locked tuning plan are more evident in terms of protecting the organs at risk. Implementing the field-locking intensity adjustment technique yields significant reductions in V5, V20, and D_{mean} for the left lung; V5 and D_{mean} for the right lung; V5 and D_{mean} for the heart; and D_{mean} for the right breast. This indicates an effective reduction in low-dose regions while maintaining target-area coverage. Although the current sample size is limited, please propose a strategy to gradually scale up the sample size according to our plan, and emphasize how to improve the prediction accuracy and optimize the service through data collection, data processing, model optimization and tuning before the sample size reaches a certain size. At the same time, please note that in the process of sample size expansion, please maintain the protection of sample privacy and comply with relevant laws and regulations on data security.

Lock field intensity modulation technology is used to better protect important organs such as the lungs and heart while ensuring normal irradiation of the target area, reducing the occurrence of complications. In the future, we will analyze the remaining organs other than PTV, left lung and heart, laying a more comprehensive theoretical foundation for clinical treatment.

Conclusion

The field locking intensity adjustment scheme can not only reduce the low dose to key organs but also has more obvious advantages in the robustness of key organs. However, the robustness of the target area needs to be improved, and the accuracy of the position needs to be improved in future treatments. In terms of dosage, current research has identified the advantages of locked in field plans in cancer.

Data Sharing Statement

All data generated or analyzed during this study are included in this published article.

Ethical/Copyright Corrections

The research complies with the Helsinki Declaration.

Ethics Approval and Consent to Participate

The present study was approved (approval no. XJZ-LL-2019-001) by the Ethics Committee of The Affiliated Cancer Hospital of Xinjiang Medical University (Urumqi, China).

Author Contributions

All authors made a significant contribution to the work reported, whether that is in the conception, study design, execution, acquisition of data, analysis and interpretation, or in all these areas; took part in drafting, revising or critically reviewing the article; gave final approval of the version to be published; have agreed on the journal to which the article has been submitted; and agree to be accountable for all aspects of the work.

Funding

The present study was supported by the Xinjiang Uygur Autonomous Region Science and Technology Support Project (grant no. 2017E0260), and by the Key Research and Development sub-project of Xinjiang Uygur Autonomous Region (grant no. 2022B03019-5);Talent echelon of Xinjiang Medical University Affiliated Cancer Hospital(RCTDAXQ).

Disclosure

The authors declare that they have no competing interests in this work.

References

1. Haga A, Magome T, Takenaka S, et al. Independent absorbed dose calculation using the Monte Carlo algorithm in volumetric modulated arc therapy[J]. *Radiat Oncol*. 2014;9(1):75. doi:10.1186/1748-717X-9-75
2. Wang W, Meng YT, L I JB, et al. Different radiotherapy plans after modified radical mastectomy for breast cancer comparative study on unplanned radiation doses in inner milk region. *Chin J Oncol*. 2018;5(40):335–340.
3. Gong HS, Meng L, Xie CB, et al. Clinical dosimetry evaluation of static IMRT with fixed jaws in specific field and VMAT for breast cancer after radical mastectomy. *Chinese Medical Equip*. 2022;4(36):113–117.
4. Michael H, Robert D, Elisabeth C, et al. Epidemiological studies of low-dose ionizing radiation and cancer: summary bias assessment and meta-analysis. *J Natl Cancer Inst Monogr*. 2020;2020(56):188–200. doi:10.1093/jncimonographs/lgaa010
5. Carver JR, Shapiro CL, Ng A; ASCO Cancer Survivorship Expert Panel. American Society of Clinical Oncology clinical evidence review on the ongoing care of adult cancer survivors: cardiac and pulmonary late effects. *J Clin Oncol*. 2007;25:3991–4008. doi:10.1200/JCO.2007.10.9777
6. Chai LY, Zhou C, Wang KF, et al. The fixed tungsten gate technology based on VMAT Application of radiotherapy after modified radical operation for left breast cancer. *Modern Oncology Learn*. 2020;28(19):3409–3413.
7. Gagliardi G, Constine LS, Moiseenko V, et al. Radiation dose volume effects in the heart. Int *J Radiat Oncol Biol Phys*. 2010;76:77–85. doi:10.1016/j.ijrobp.2009.04.093
8. Darby SC, Ewertz M, McGale P, et al. Risk of ischemic heart disease in women after radiotherapy for breast cancer. *N Engl J Med*. 2013;368(11):987–988. doi:10.1056/NEJMoa1209825

9. Afifi AM, Saad AM, Al-Husseini MJ, et al. Causes of death after breast cancer diagnosis: a US population-based analysis[J]. *Cancer*. 2020;126:1559–1567. doi:10.1002/cncr.32648
10. Jacobse JN, Duane FK, Boekel NB, et al. Radiation dose-response for risk of myocardial infarction in breast cancer survivors. *Int J Radiat Oncol Biol Phys*. 2019;103:595–604. doi:10.1016/j.ijrobp.2018.10.025
11. Jacob S, Camilleri J, Derreumaux S, et al. Is mean heart dose a relevant surrogate parameter of left ventricle and coronary arteries exposure during breast cancer radiotherapy: a dosimetric evaluation based on individually-determined radiation dose (BACCARAT study). *Radiat Oncol*. 2019;14:29. doi:10.1186/s13014-019-1234-z
12. Yock AD, Mohan R, Flampouri S, et al. Robustness analysis for external beam radiation therapy treatment plans: describing uncertainty scenarios and reporting their dosimetric consequences. *Pract Radiat Oncol*. 2019;9:200–207. doi:10.1016/j.prro.2018.12.002
13. Ding Z, Xiaoyong X, Chenbin L, et al. Evaluation of plan robustness using hybrid intensity-modulated radiotherapy (IMRT) and volumetric arc modulation radiotherapy (VMAT) for left-sided breast cancer. *Bioengine*. 2022;9:131–145. doi:10.3390/bioengineering9040131
14. Jan U, Markus A, Mark B, et al. Robust radiotherapy planning. *Phys Med Biol*. 2018;63:1–48.
15. Oskar E, Tianfang Z. Robust automated radiation therapy treatment planning using scenario-specific dose prediction and robust dose mimicking. *Medic Physics*. 2022;49(5):3564–3573.
16. Shouyi W, Haibo L, Minglei K, et al. Dose rate and dose robustness for proton transmission FLASHRT treatment in lung cancer. *Original Res*. 2022;8:1–11.
17. Wennstig AK, Wadsten C, Garmo H, et al. Long-term risk of ischemic heart disease after adjuvant radiotherapy in breast cancer: results from a large population-based cohort. *Breast Cancer Res*. 2020;22:10. doi:10.1186/s13058-020-1249-2
18. Wennstig AK, Garmo H, Isacsson U, et al. The relationship between radiation doses to coronary arteries and location of coronary stenosis requiring intervention in breast cancer survivors[J]. *Radiat Oncol*. 2019;14:40. doi:10.1186/s13014-019-1242-z
19. Chung SY, Oh J, Chang JS, et al. Risk of cardiac disease in patients with breast cancer: impact of patient-specific factors and individual heart dose from three-dimensional radiation therapy planning. *Int J Radiat Oncol Biol Phys*. 2021;110:473–481. doi:10.1016/j.ijrobp.2020.12.053
20. Nairooz R, Kundu A, Chatterjee S. Bangalore S. Long-term cardiovascular mortality after radiotherapy for breast cancer: a systematic review and meta-analysis. *Clin Cardiol*. 2017;40:73–81. doi:10.1002/clc.22631
21. Yun-Jiu C, Xiao-Ying N, Cheng-Cheng J, et al. Long-term cardiovascular risk after radiotherapy in women with breast cancer. *J Am Heart Assoc*. 2017;6. doi:10.1161/JAHA.117.005633
22. Drost L, Yee C, Lam H, et al. A systematic review of heart dose in breast radiotherapy. *Clin Breast Cancer*. 2018;18:19–24. doi:10.1016/j.clbc.2018.05.010
23. Alessandro T, Stefano C, Giulia V, et al. Deep inspiration breath-hold intensity modulated radiation therapy in a large clinical series of 239 left-sided breast cancer patients: a dosimetric analysis of organs at risk doses and clinical feasibility from a single center experience. *Br J Radiol*. 2019;92(1101):20190150. doi:10.1259/bjr.20190150
24. Zhang X, Rong Y, Morrill S, et al. Robust optimization in lung treatment plans accounting for geometric uncertainty [J]. *Appl Clin Med Phys*. 2018;19:19–26. doi:10.1002/acm2.12291
25. Dunlop A, Colgan R, Kirby A, et al. Evaluation of organ motion-based robust optimization for VMAT planning for breast and internal mammary chain radiotherapy[J]. *Clin Transl Radiat Oncol*. 2019;16:60–66. doi:10.1016/j.ctro.2019.04.004